ELSEVIER

Journal of Power Sources 102 (2001) 224–232

JOURNAL OF POWER SOURCES

www.elsevier.com/locate/jpowsour

The effect of Cd, Co, and Zn as additives on nickel hydroxide opto-electrochemical behavior

K. Provazi[a], M.J. Giz[b], L.H. Dall'Antonia[a], S.I. Córdoba de Torresi[a,*]

[a]*Departameno de Quimica Fundamental, Instituto de Química, Universidade de São Paulo, C.P. 26077, 05513-970 São Paulo (SP), Brazil*
[b]*Instituto de Química de São Carlos, Universidade de São Paulo, C.P. 780, 13560-970 São Carlos (SP), Brazil*

Received 12 March 2001; accepted 19 April 2001

Abstract

Nickel hydroxide films were coprecipitated with the additives $Cd(OH)_2$, $Co(OH)_2$, and $Zn(OH)_2$ by galvanostatic electrodeposition process. The effects of the $Cd(OH)_2$, $Co(OH)_2$, and $Zn(OH)_2$ additions on electrode properties such as charge–discharge, reversibility of the electrode reaction, espectroelectrochemical behavior, superficial morphology by atomic force microscopy (AFM) images, were studied. An anomalous coprecipitation of $Zn(OH)_2$ was observed. The different concentration of zinc nitrate on the solution affects the amount of zinc hydroxide found on the film; this behavior must be attributed to the differences on the solubility products (K_{ps}) of the nickel and zinc hydroxides and also to the remarkable zinc amphoteric character. All additives studied displaced the oxygen evolution reaction (OER) to more positive values, and reduced the difference between the oxidation and reduction peaks (Ni(II)/Ni(III)), leading to an augmentation of the process reversibility. However, a significant loss on the electrode efficiency was observed for composite films with zinc. Lithium hydroxide solution as electrolyte showed an augmentation of the difference between the peak potential for the oxidation process and the oxygen evolution reaction, and also increased the reversibility of the redox nickel process. AFM images showed similar superficial morphologies for nickel hydroxide films and films with cobalt; on the other hand, films containing cadmium and zinc showed an inhomogeneous morphology. Nickel hydroxide film shows a differentiated spectroelectrochemical behavior when compared with composite films.

Keywords: Nickel hydroxide; Cadmium hydroxide; Cobalt hydroxide; Zinc hydroxide; Additives; Electrochromism

1. Introduction

Nickel hydroxide is commonly used as an active material for nickel positive electrodes in Ni-based rechargeable batteries [1–6], electrochromic devices [7], and as promising catalysts for oxygen evolution reaction (OER) [8,9]. Some properties of nickel hydroxide electrodes (such as high power density, very good cyclability, and high specific energy) have made them very viable for an extended range of applications. It is reported that there are four phases produced over the lifetime of a nickel hydroxide electrode, namely α-$Ni(OH)_2$, γ-NiOOH, β-NiOOH, and β-$Ni(OH)_2$ and the electrochemical reactions of nickel hydroxides can be shown simply by [10]

$$\begin{array}{ccc} \alpha\text{-Ni(OH)}_2 & \rightleftarrows & \gamma\text{-NiOOH} \\ \downarrow & & \uparrow \\ \beta\text{-Ni(OH)}_2 & \rightleftarrows & \beta\text{-NiOOH} \end{array}$$

In a battery application, $\alpha \leftrightarrow \gamma$ cycling has a couple of advantages over $\beta \leftrightarrow \beta$ cycling. First, more electrons are exchanged per nickel atom in the $\alpha \leftrightarrow \gamma$ cycling, because the oxidation state of nickel in γ-NiOOH is higher than that of β-NiOOH [11,12]. The formation of γ-NiOOH is associated with the volume expansion or swelling of the nickel hydroxide electrode. The phase change from β-NiOOH to γ-NiOOH can be correlated to a 44% increase in volume [13,14]. Kamath et al. reported that a stabilized α-$Ni(OH)_2$ electrode has a much larger charge capacity than a β-$Ni(OH)_2$ electrode [12].

Second, on prolonged charging, β-NiOOH is known to be converted to γ-NiOOH, causing a mechanical deformation which results in an irreversible damage to the electrode [15]. On the other hand, α-$Ni(OH)_2$ can be cycled to γ-NiOOH reversibly without any mechanical deformation [11,12]. Therefore, α-$Ni(OH)_2$ is expected to be a better electroactive material for a high-performance nickel positive electrode.

The presence of certain metal cations in hydrated nickel oxides and oxyhydroxides, generically referred as nickel hydrous oxides, can strongly affect the electrochemical

* Corresponding author. Fax: +55-11-3815-5579.
E-mail address: storresi@quim.iq.usp.br (S.I. Córdoba de Torresi).

0378-7753/01/$ – see front matter
PII: S0378-7753(01)00819-9

characteristics of this interesting electrode material [2]. Cobalt, cadmium, and zinc are commonly used as beneficial additives in nickel battery electrodes [16–21]. The addition of several percent of additives such as Cd, Co, and Zn to the nickel hydroxide is a very effective method of suppressing the formation of γ-NiOOH [22]. Although, there are numerous studies on these topics, the results are still not complete.

In the present work, thin nickel hydroxide films were prepared by electroprecipitation. The influence of the coprecipitated additives such as $Cd(OH)_2$, $Co(OH)_2$, and $Zn(OH)_2$ in different percentages on the characteristics of the electrodes was also studied for the purpose of increasing the electrochemical activity of the active material, and two electrolytes were used, KOH and LiOH. Atomic force microscopy (AFM) images of the electrode were obtained revealing the superficial morphology changes for different composite films. Moreover, espectroelectrochemical measurements were carried out showing the effect of the additives on films electrochromic behavior.

2. Experimental

2.1. Film deposition

Composite films were prepared by cathodic electrodeposition from a 0.01 mol/l $Ni(NO_3)_2$ solution with different amounts of $M(NO_3)_2$, where $M = Co^{2+}$, Cd^{2+}, and Zn^{2+}. The proportion of M used was 5 and 10% in solution. Deposition was carried out galvanostatically by the application of a current density of -0.1 mA/cm^2 for 200 s (20 mC/cm^2).

2.2. Substrates

Substrates were glass pieces (1.0 cm × 3.0 cm) with a conductive coating of ITO (Delta Technologies, $R \leq 20\ \Omega/\square$). Prior to use, substrates were degreased by cleaning with detergent soap and acetone, subsequently rinsed with distilled water. A pretreatment of the substrate was performed by applying a current (∼2 mA/cm^2) for 10 s in a 1 mol/l NaOH aqueous solution. This procedure leads to more homogenous electrodeposited films.

2.3. Spectroelectrochemical cell and electrodes

Working electrodes were placed in a rectangular acrylic cell. The counter electrode was a platinum wire and all potentials were referred to saturated calomel reference electrode (SCE). The cell contained about 50 ml of 1 mol/l KOH electrolytic solution prepared from analytical grade KOH and purified water (Elga System UHQ).

2.4. Instrumentation

Electrochemical measurements were performed under potentiodynamic and potentiostatic conditions with a potentiostat Autolab PGSTAT 30 by Ecochimie. The electric charge was recorded simultaneously with the change of monochromatic or polychromatic transmittance, which was followed by placing the electrochemical cell in the optical pathway of a HP8453 diode array spectrophotometer.

Films and solutions chemical compositions were obtained using an inductively coupled plasma atomic emission spectrophotometer (ICP-AES; Spectroflame Modula Segmental-Spectro Co. equipment). All ICP-AES determinations were performed by triplicate.

The AFM measurements were carried out at room temperature and room humidity, using a TopoMetrix 2010 instrument. The non-contact mode was used for taking topographic images. The amplitude frequencies were around 340 kHz. A 7 μm scanner and commercial etched silicon tips were employed during the morphology evaluations. The mean spring constant of the tips was 34.0–58.0 N/m, the length was 120 μm, and the tip ends were about 10–15 nm in diameter. The samples were attached to the sample holder with conductive carbon double-side tape. The images are mainly raw data except that in some cases, minor flatness and tilt corrections have been made. The working temperature during electrochemical experiments was 25°C.

3. Results and discussion

3.1. Chemical composition of nickel hydroxide films

Electrochromic mixed hydroxide films were deposited by cathodic deposition from mixed metal nitrate solutions. In this process [23,24], the reduction of nitrate to ammonium produces hydroxyl ions, increasing the pH at the electrode surface. By this way, metal ions will react to precipitate metal hydroxides according to the following reactions:

$$NO_3^- + 7H_2O + 8e^- \rightarrow NH_4^+ + 10OH^- \quad (1)$$

$$M^{n+} + nOH^- \rightarrow M(OH)_n \quad (2)$$

where M^{n+} is Ni^{2+} or Co^{2+}, Cd^{2+}, and Zn^{2+}. The amount of additive in the deposition solution used was 5 and 10% in order to obtain different film compositions, once the electrochemical and optical properties strongly depend on the amount of these additives. The chemical compositions of the solution before electrodeposition were determined by ICP-AES and are shown in Table 1. A small difference can be

Table 1
Chemical composition of the nickel nitrate solutions plus additives

Additive	Additive calculated (%)	Additive determined (%)
Cd	5	3.3 ± 0.2
Cd	10	7.6 ± 0.4
Co	5	4.2 ± 0.2
Co	10	9.6 ± 0.5
Zn	5	7.6 ± 0.4
Zn	10	12.0 ± 0.6

Table 2
Chemical composition of the nickel hydroxide films plus additives

Additive	Additive expected (%)	Additive determined (%)
Cd	3.3	2 ± 1
Cd	7.6	7 ± 1
Co	4.2	5 ± 1
Co	9.6	6 ± 1
Zn	7.6	1.0 ± 0.4
Zn	12.0	47 ± 2

observed between the values calculated and those determined. These differences are due to errors during manipulation of the reagents, different salt hydration, and others.

After the electrodeposition of the films, new ICP-AES experiments were carried out to confirm the real composition of the films. The measurements were done by dissolving the film in 5 ml of concentrated nitric acid. The results are showed in Table 2.

A slight difference can be observed between the values of the real chemical composition in the precursor solutions (Table 1) and those observed in the films with the additives Cd and Co. This fact could be related to the different solubility products (K_{ps}) of the hydroxides: $K_{ps}[Ni(OH)_2] = 5.47 \times 10^{-16}$; $K_{ps}[Cd(OH)_2] = 5.27 \times 10^{-15}$; $K_{ps}[Co(OH)_2] = 5.92 \times 10^{-15}$ [25]. As it is observed, the K_{ps} values for the additives are bigger than nickel hydroxide's one; so that, the preferential deposition of $Ni(OH)_2$ related to the additives would be expected. Experimental results showed in Table 2 confirm this statement.

A particular behavior is observed for the composition determined in the films with Zn as additive. When the precursor solution contains 7.6% Zn, the resulting electrodeposited film has just a small amount of 1.1% Zn in its composition. Once the value of $K_{ps}[Zn(OH)_2] = 5.24 \times 10^{-24}$, that is to say, at least eight magnitude order smaller than the value of nickel hydroxide K_{ps}, a huge precipitation of zinc hydroxide instead of nickel hydroxide should be expected. As mentioned before, on the interface between substrate and solution, during the electrodeposition of the hydroxides, the pH increases drastically due the reduction of nitrate to ammonium producing hydroxyl ions, reaction (1), and it is expected that the precipitation of the hydroxide in the case of Zn is as follows:

$$Zn^{2+} + 2OH^- \rightleftarrows Zn(OH)_{2\,(s)} \quad (3)$$

If the increase of surface OH^- concentration is very high, the well-known amphoteric character of zinc should lead to the formation of soluble species such as $[Zn(OH)_4]^{2-}_{(aq)}$, as shown in the following reaction (4):

$$Zn^{2+} + 4OH^- \rightleftarrows [Zn(OH)_4]^{2-}_{(aq)} \quad (4)$$

As it can be observed from ICP-AES results, the amount of zinc is very low from that we should expect, and the precipitation of the zinc hydroxide is not occurring due to the soluble complex formation.

On the other hand, an increase of the Zn concentration in the solution leads to a resulting film with large amount of Zn. In this case, increasing the amount of zinc in the solution and consequently, in the interface, the formation of soluble species is reduced and the preferential precipitation of the hydroxide takes place. Additionally, the big difference between zinc and nickel hydroxide's K_{ps} would explain the deposition of zinc hydroxide in a bigger amount than nickel hydroxide, leading to a final film composition corresponding to a mixture of zinc and nickel hydroxide in the proportion of 1:1.

3.2. Surface image

The AFM surface images of nickel hydroxide electrodes without additives and composite films with 7% Cd, 6% Co, and 47% Zn are shown in Fig. 1. Deposits containing Co as additive (Fig. 1(B)) produces homogenous films. When this film is compared with the nickel hydroxide one (Fig. 1(A)), even a homogeneous surface morphology can be observed and it presents some particular differences from the nickel hydroxide without additives electrode image. Also, from the images can be inferred that a strong physical interaction exists between the individual components and consequently the formation of a solid solution, as suggested in the literature [26]. It is also well known that the coelectrodeposition of Ni and Co hydroxides generates a mixed single-phase metal hydrous oxide in which Co ions occupy Ni sites in the lattice, and not two intermixed phases, each consisting of a single metal hydrous oxide [27]. Also, this excellent interaction between Ni and Co hydroxides could be explained by some similarities of these two elements: not only the ionic radii is very close (0.69 Å for Ni^{2+} and 0.63 Å for Co^{2+} [25]), but also the bond strengths of the cations with the oxygen (382.0 and 384.5 kJ/mol for Ni–O and Co–O [25], respectively) are also similar.

Fig. 1(C) and (D) shows the micrographs of films containing 7% Cd and 47% Zn, respectively. These films were found to consist of conformal sections covered by large number of distinctly bright, globular-type features, separated by sharply defined crevices. Remarkable differences can also be observed on the properties of the Cd and Zn cations compared with Ni ones: not only the ionic radii of the additives (0.74 Å for Zn^{2+} and 0.97 Å for Cd^{2+} [25]) are very different from ionic radius of nickel cation (0.69 Å for Ni^{2+} [25]), but also bond strengths of the cations with oxygen (270.7, 235.6, and 382.0 kJ/mol for Zn–O, Cd–O, and Ni–O [25], respectively). These features could result in different morphologies that could be related to low interaction between nickel sites and those of the additives. AFM images of composite films with Zn and Cd as additives clearly show a less compact structure leading to a higher active area of these electrodes that should affect optical and electrochemical behavior. The morphology and structure of the nickel hydroxide films displayed a particular role on the

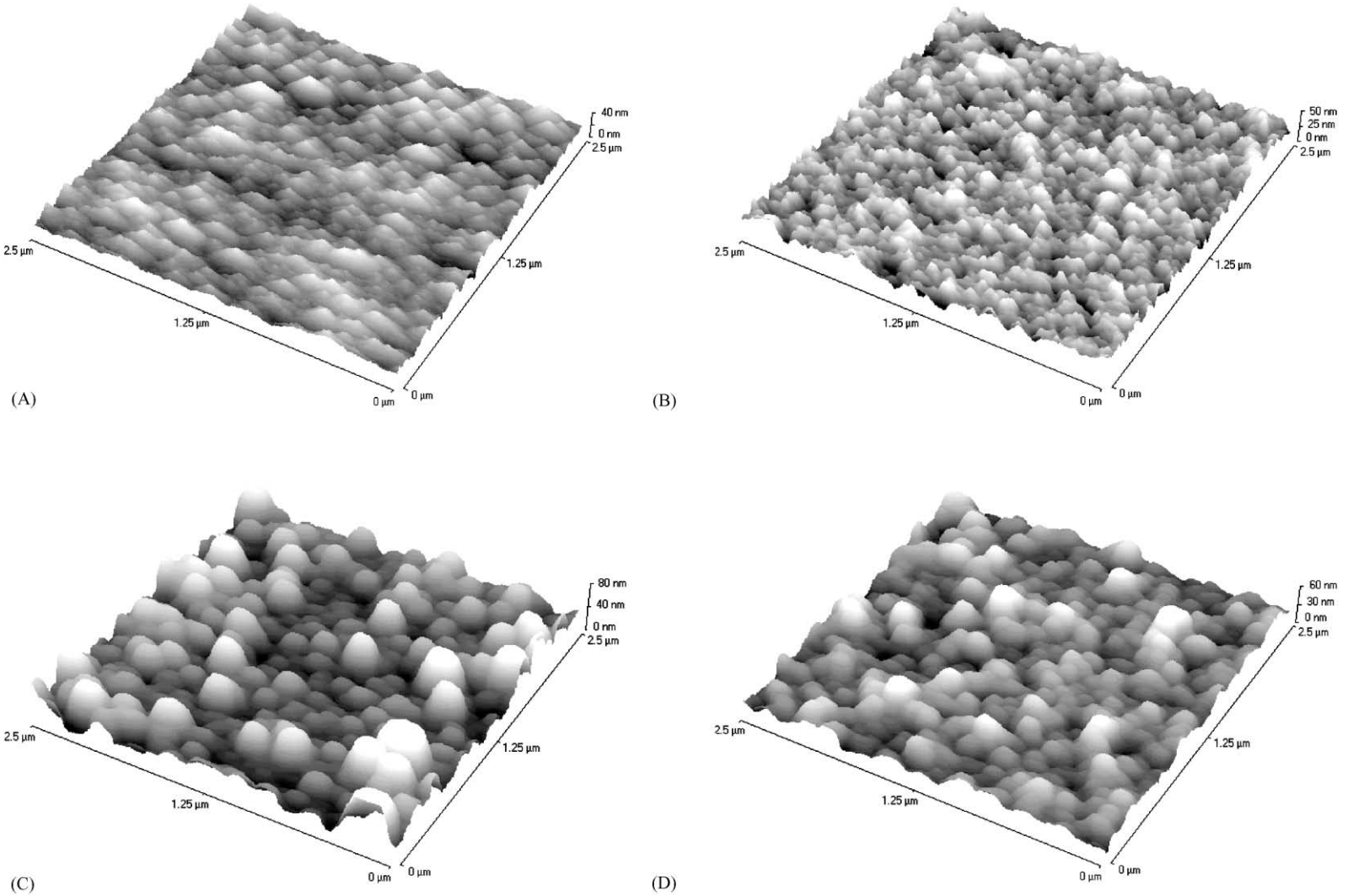

Fig. 1. AFM images of a 2.5 µm × 2.5 µm area of different films as prepared, reduced state, supported on ITO: (A) $Ni(OH)_2$ film; (B) $Ni(OH)_2$ + 5.6 wt.% $Cd(OH)_2$ composite film; (C) $Ni(OH)_2$ + 6.8 wt.% $Co(OH)_2$ composite film; (D) $Ni(OH)_2$ + 47.0 wt.% $Zn(OH)_2$ composite film.

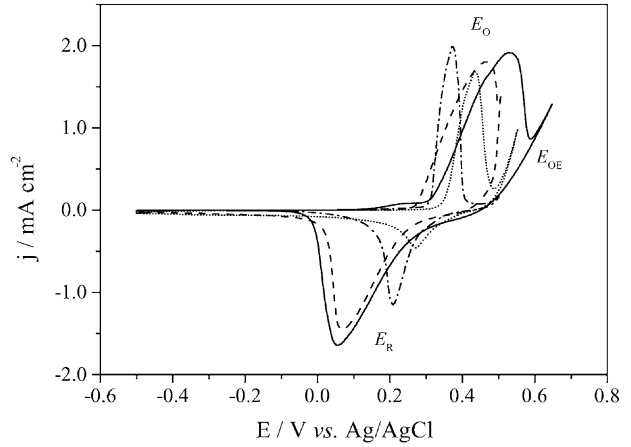

Fig. 2. Cyclic voltammograms for nickel hydroxide and composite of various composition electrodes electrodeposited on ITO in 1 mol/l KOH solution (scan rate: 10 mV/s). The first cycle of each electrode was recorded: (—) $Ni(OH)_2$ film; (- - -) $Ni(OH)_2 + 4.6$ wt.% $Cd(OH)_2$ composite film; (-·-·-·) $Ni(OH)_2 + 2.3$ wt.% $Co(OH)_2$ composite film; (· · ·) $Ni(OH)_2 + 1.1$ wt.% $Zn(OH)_2$ composite film.

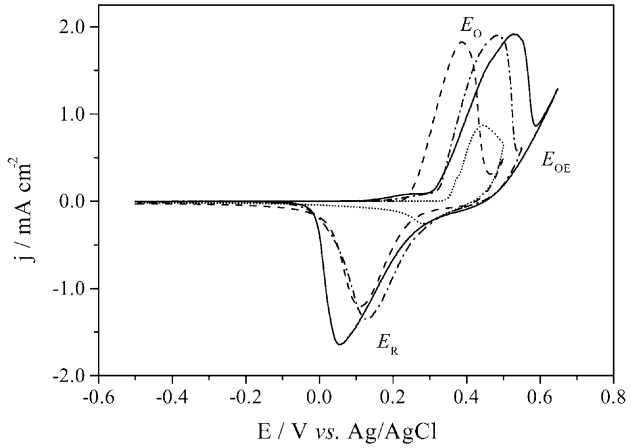

Fig. 3. Cyclic voltammograms for nickel hydroxide and composite of various composition electrodes electrodeposited on ITO in 1 mol/l KOH solution (scan rate: 10 mV/s). The first cycle of each electrode was recorded: (—) $Ni(OH)_2$ film; (- - -) $Ni(OH)_2 + 5.6$ wt.% $Cd(OH)_2$ composite film; (-·-·-·) $Ni(OH)_2 + 6.8$ wt.% $Co(OH)_2$ composite film; (· · ·) $Ni(OH)_2 + 47.0$ wt.% $Zn(OH)_2$ composite film.

charge/discharge behavior, affecting the proton diffusion coefficient value, $\tilde{D}$, and consequently producing differences on the films behavior [28].

3.3. Electrochemical properties

3.3.1. Cyclic voltammograms

The electrochemical behavior of the $Ni(OH)_2$ electrode has been extensively investigated [29–31]. A cyclic voltammogram for $Ni(OH)_2$ prepared by electrochemical deposition is shown in Fig. 2. The two current peaks at 0.533 and 0.053 V correspond to the redox couple Ni(II)/Ni(III). The overall electrode reaction constitutes the basis for the operation of the Ni oxide electrode in rechargeable battery application [31] and it can be described as

$$Ni(OH)_2 + OH^- \rightleftarrows NiOOH + H_2O + e^- \quad (5)$$

Figs. 2 and 3 show cyclic voltammograms for different composite electrodes obtained in the first cycle. The experimental results relating the profile of the voltammograms are outlined in Table 3. The reversibility of the electrode reaction can be measured by the difference ($E_O - E_R$) between the oxidation potential (E_O) and the reduction potential (E_R). However, the efficiency of the electrode could be related to the accomplishment of a full reduction of the film, plainly the oxidation charge (Q_O) must be the same of the reduction charge (Q_R), consequently the ratio Q_O/Q_R is close to 1. On the other hand, if the reduction charge is smaller than the oxidation charge, a loss in the efficiency is observed and a deviation from 1 is obtained in the ratio Q_O/Q_R. It can be seen from Table 3 that the reversibility for electrode reaction is significantly improved by the additions of Co, Cd, and Zn. Particularly, the electrode with 2% Cd shows the lowest oxidation potential and the most reversible behavior. Also Zn addition promotes a diminution of the difference $E_O - E_R$, implying a good reversibility, but the ratio Q_O/Q_R has a large deviation from 1, indicating a drop in the charge efficiency of the electrode.

A large difference ($E_{OE} - E_O$) between the oxygen evolution (E_{OE}) and the oxidation potentials (E_O) is beneficial for nickel electrodes. Although, the oxygen evolution reaction shifts to less positive values, the difference ($E_{OE} - E_O$) became bigger for the composite films than pure nickel hydroxide ones. Overwhelmingly the additives support an increase in the difference between E_{OE} and E_O and allow the electrodes to be fully charged, that means the complete oxidation of Ni^{2+} to Ni^{3+} [32]. Consequently, long cyclability and larger capacity are properties that should be expected for electrodes containing additives. From the values summarized in Table 3, it can be seen that the best electrode performance is shown for films with 3% Cd. Since the difference ($E_{OE} - E_O$) is the largest observed and also this

Table 3
Oxidation potential (E_O), reduction potential (E_R), oxygen evolution potential (E_{OE}), the difference between E_O and E_R, the difference between E_{OE} and E_O, and the ratio between the oxidation and reduction charges (Q_O and Q_R, respectively) for various composite nickel electrodes

Additive	Additive (%)	Potential values (V)					
		E_O	E_R	E_{OE}	$E_O - E_R$	$E_{OE} - E_O$	Q_O/Q_R
Ni	Pure	0.533	0.053	0.589	0.480	0.056	0.97
Cd	2	0.372	0.209	0.483	0.163	0.111	0.99
Cd	7	0.482	0.131	0.538	0.351	0.056	1.03
Co	5	0.465	0.066	0.524	0.399	0.059	0.95
Co	6	0.387	0.111	0.462	0.276	0.075	0.98
Zn	1	0.436	0.271	0.487	0.165	0.051	1.63
Zn	47	0.44	0.288	0.502	0.152	0.062	1.97

electrode shows the smallest value of $E_O - E_R$, confirming a great reversibility of the redox process.

3.3.2. Cycle life

The durability of the electrodes could be followed by the number of charge and discharge cycles. As should be expected, the cycle lives of the electrodes are related to the chemical nature of the additives and the longest cycle life was achieved for the electrode containing 7% Co^{2+} additive. For these composite films, after 200 charge–discharge cycles, the electrode still retained 10% of its initial capacity, a higher value than that for any other electrode that retained only 5% or less of the initial capacity.

3.3.3. The electrolyte effect

With the aim of investigating the effect of the electrolyte on the composite nickel electrode behavior, different composite films were cycled in a 1.0 mol/l LiOH. Figs. 4 and 5 show the cyclic voltammetry of the films with additives in LiOH solution and the electrochemical results are summarized in Table 4. Remarkable changes are observed regarding reversibility of the electrodes when the electrolyte is changed to LiOH; specifically, the difference $E_O - E_R$ became smaller with the change of the electrolyte, this fact is assigned to the retained lithium by the active material and consequently formation of a new composite where the lithium plays a role as an additive [33–35]. All the films with different additives follow this behavior.

Although, the oxygen evolution reaction onset is always at the same value of potential, for nickel pure or composite electrodes, in lithium hydroxide electrolyte, the difference ($E_{OE} - E_O$) is bigger for the composite electrodes than for pure nickel hydroxide due the shift of oxidation peak potential to less positive values. Once again, the electrode efficiency is improved.

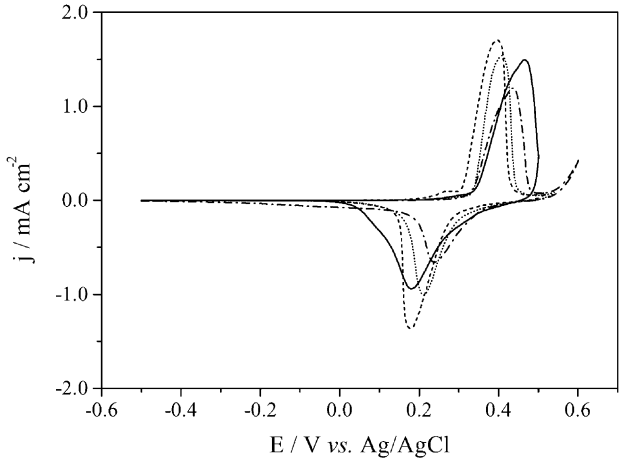

Fig. 4. Cyclic voltammograms for nickel hydroxide and composite of various composition electrodes electrodeposited on ITO in 1 mol/l LiOH solution (scan rate: 10 mV/s). The first cycle of each electrode was recorded: (—) $Ni(OH)_2$ film; (- - -) $Ni(OH)_2 + 4.6$ wt.% $Cd(OH)_2$ composite film; (-·-·-·-) $Ni(OH)_2 + 2.3$ wt.% $Co(OH)_2$ composite film; (· · ·) $Ni(OH)_2 + 1.1$ wt.% $Zn(OH)_2$ composite film.

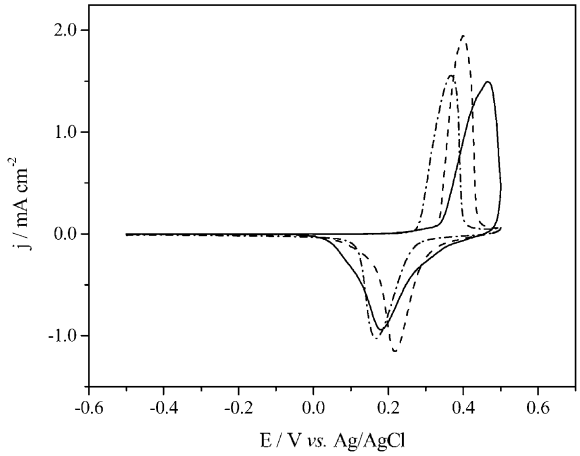

Fig. 5. Cyclic voltammograms for nickel hydroxide and composite of various composition electrodes electrodeposited on ITO in 1 mol/l LiOH solution (scan rate: 10 mV/s). The first cycle of each electrode was recorded: (—) $Ni(OH)_2$ film; (- - -) $Ni(OH)_2 + 5.6$ wt.% $Cd(OH)_2$ composite film; (-·-·-·-) $Ni(OH)_2 + 6.8$ wt.% $Co(OH)_2$ composite film.

3.4. Spectroelectrochemistry

Potential changes affect the optical properties of nickel hydroxide thin films. The color of the film is related to the oxidation state of nickel hydroxide. Previous work [36] has shown that nickel hydroxide in the reduced state is transparent, no absorption band appears in the visible region, and the electrode transmits ca. 75% ($\lambda = 450$ nm). However, in the oxidized state, the electrode becomes dark brown colored with a transmittance of 3%. Changes in morphology and composition of the films provoked by the additives should interfere with the optical response of the electrodes and this influence has been investigated and the results are described below.

Fig. 6 shows absorption spectra obtained with $Ni(OH)_2$ and $Ni(OH)_2 + 6\%$ $Cd(OH)_2$ electrodes at different polarization potentials. It is possible to infer that the optical spectra of $Ni(OH)_2$ film have not been changed because of the presence of the additive, but the optical contrast measured was ca. 55% ($\lambda = 520$ nm) in transmittance. In spite of

Table 4
Summarized electrochemical results for composite nickel electrodes in lithium hydroxide electrolyte, difference between oxidation potential (E_O) and reduction potential (E_R), difference between oxygen evolution potential (E_{OE}) and E_O, and the ratio between oxidation and reduction charges (Q_O and Q_R, respectively) for various composite nickel electrodes

Additive	Additive (%)	Potential values (V)		
		$E_O - E_R$	$E_{OE} - E_O$	Q_O/Q_R
Ni	Pure	0.249	0.083	1.08
Cd	2	0.215	0.118	1.10
Cd	7	0.198	0.117	1.16
Co	5	0.196	0.117	0.94
Co	6	0.181	0.081	1.08
Zn	1	0.196	0.089	1.08

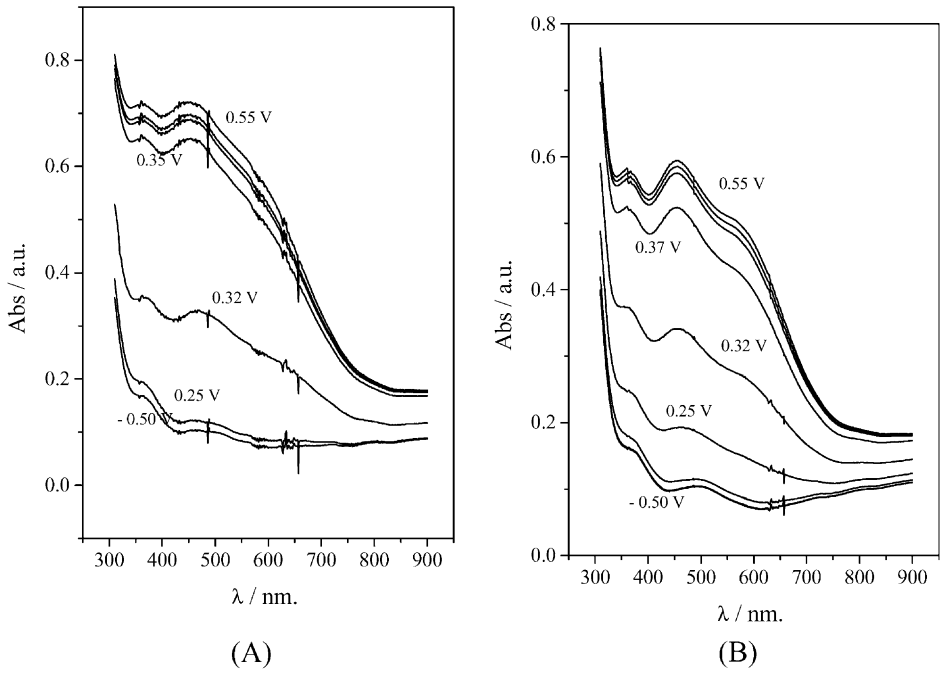

Fig. 6. Absorption spectra obtained at different potentials for: (A) $Ni(OH)_2$ film; (B) $Ni(OH)_2$ + 5.6 wt.% $Cd(OH)_2$ composite film.

the fact that the presence of cadmium in the composite leads to the formation of a film with a lower contrast, the potential where the colored state is reached is less positive for the composite film. It must be pointed out that, even smaller than pure $Ni(OH)_2$, the contrast obtained is excellent for practical applications. It must be emphasized that during these experiments, the potential was held for a period of time while the acquisition of data was carried out, and it was not made by a linear sweep voltammetry.

In a similar way, to the composite film with Cd, films containing Co as additive still did not show a particular feature (Fig. 7(A)) that differs from the nickel hydroxide film and the spectra shows that the color change is shifted to less positive potentials, albeit the optical contrast is

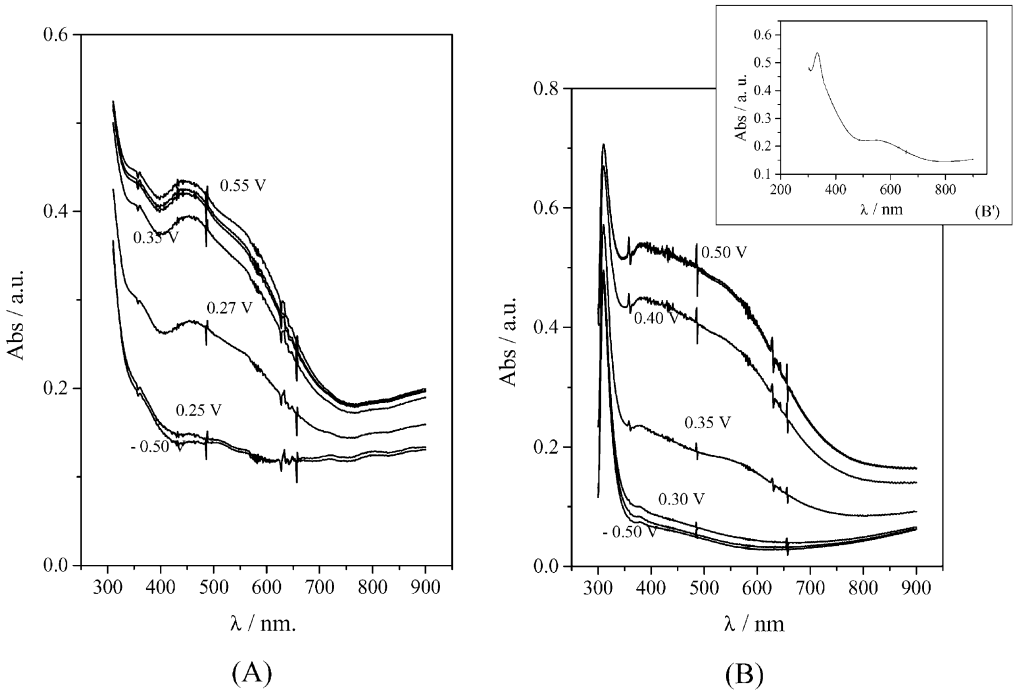

Fig. 7. Absorption spectra obtained at different potentials for: (A) $Ni(OH)_2$ + 6.8 wt.% $Co(OH)_2$ composite film; (B) $Ni(OH)_2$ + 1.1 wt.% $Zn(OH)_2$ composite film (inset (B′): $Zn(OH)_2$ film).

smaller compared with other electrodes, ca. 30%. This behavior illustrated that even the reversibility of the electrodes containing Co is improved, the optical contrast is not high showing poorer optical properties than composites with Cd.

Changes can be observed for spectra of electrodes containing Zn as additive (1.1%) (Fig. 7(B)), where a new band appears at ca. 325 nm. The inset Fig. 7(B′) shows the absorption spectra of a pure $Zn(OH)_2$ film prepared by galvanostatic precipitation from a $Zn(NO_3)_2$ solution. As can be seen, the same band is observed in pure $Zn(OH)_2$ films, suggesting that it could be related to zinc species. The optical contrast observed with these composite electrodes was around 63%. Although, this value is the highest one found among all the electrodes studied, this film presents a great problem that must be overcome: the electrode is not reversible and in the second cycle the efficiency and the optical contrast dropped by half.

4. Conclusions

By coprecipitating Cd, Co, and Zn in nickel hydroxide films, the final composite electrode prepared are in the forms of $(Ni, Cd)(OH)_2$, $(Ni, Co)(OH)_2$, and $(Ni, Zn)(OH)_2$ with different percentages of additives. The film composition changed with the additives, and coprecipitation of Cd and Co occurred as expected, the amounts of salt in the solution were close to the quantities of additives found in the film by ICP-AES, but for Zn the results were different. For small quantities of Zn in solution (5%), the resulting film has a very little zinc hydroxide precipitated (1%) as a result of the amphoteric zinc character forming a soluble complex in the substrate–solution interface due to the high concentration of OH^- species. On other hand, if the amount of zinc in solution is increased (10%), the additive coprecipitation is much higher (ca. 47%) than predicted.

Composite films with Co showed a very compact structure and similar to nickel hydroxide films, revealed by the AFM images, as expected due to the similar physical properties of the Co^{2+} and Ni^{2+} ions. However, films with Cd and Zn as additives present very distinct superficial morphology from that of nickel hydroxide films, with globular-type features separated by crevices. This is expected since the additives physical properties (e.g. ionic radii) are very different from nickel hydroxide.

Electrodes with 2% Cd showed the lowest oxidation potential and the most reversible behavior. In the first cycle also Zn additions promote a diminution of the difference between the oxidation and reduction potentials, but the efficiency of the electrode drops for subsequent cycles due to incomplete reduction of the electrode. The additives also promote a displacement of the oxygen evolution potential to more positive values.

Spectroelectrochemical experiments revealed that composite films still keep the electrochromic behavior of the nickel hydroxide thin film, showing acceptable optical parameters for practical applications.

Acknowledgements

The authors would like to thank the FAPESP (98/7624-8; 98/15675-1; 99/09583-0) and CNPq for financial support. Dr. E. de Oliveira (IQ-USP) is gratefully acknowledged for ICP-AES measurements.

References

[1] J. Desilvestro, O. Haas, J. Electrochem. Soc. 137 (1990) 5C.
[2] J. McBreen, in: R.E. White, J.O.M. Bockris, B.E. Conway (Eds.), Modern Aspects of Electrochemistry, Vol. 21, Plenum Press, New York, 1990, p. 29.
[3] G. Halpert, in: D.A. Corrigan, A.H. Zimmerman (Eds.), Nickel Hydroxide Electrodes, PV 90-4, The Electrochemical Society Proceedings Series, Pennington, NJ, 1990, p. 1.
[4] F. Portemer, A. Delahaye-Vidal, M. Figlarz, J. Electrochem. Soc. 139 (1992) 671.
[5] I. Krejcí, P. Vanýsek, J. Power Sources 47 (1994) 79.
[6] C. Delmas, C. Faure, L. Gautier, L.G. Demourgues, A. Rougier, Philos. Trans. R. Soc. Lond. Ser. A 354 (1996) 1545.
[7] T. Maruyama, S. Arai, J. Electrochem. Soc. 143 (1996) 1383.
[8] I. Nikolov, R. Darkaoui, E. Zhecheva, R. Stoyanova, N. Dimitrov, T. Vitanov, J. Electroanal. Chem. 429 (1997) 157.
[9] S.I. Cordoba, R.E. Carbonio, M. Lopez Teijelo, V.A. Macagno, Electrochim. Acta 31 (1986) 1321.
[10] H. Bode, K. Dehmelt, J. Witte, Electrochim. Acta 11 (1966) 1079.
[11] C. Faure, C. Delmas, M. Fouassier, J. Power Sources 35 (1991) 279.
[12] P.V. Kamath, M. Dixit, L. Indira, A.K. Shukla, V.G. Kumar, N. Munichandraiah, J. Electrochem. Soc. 141 (1994) 2956.
[13] D. Singh, J. Electrochem. Soc. 145 (1998) 116.
[14] A. Kowal, R. Niewiara, B. Peronczynk, J. Haber, Langmuir 12 (1996) 2332.
[15] N. Sac-Epée, M.R. Palacin, A. Delahaye-Vidal, Y. Chabre, J.-M. Tarâscon, J. Electrochem. Soc. 145 (1998) 1434.
[16] M. Oshitani, H. Yufu, K. Takasima, S. Tsuji, Y. Matsumaru, J. Electrochem. Soc. 136 (1989) 1590.
[17] R.D. Armstrong, J. Power Sources 25 (1989) 89.
[18] D.H. Fritts, J. Electrochem. Soc. 129 (1982) 118.
[19] W. Lee, J. Electrochem. Soc. 132 (1985) 2835.
[20] M.E. Uñates, E. Folquer, J.R. Vilche, A.J. Arvia, J. Electrochem. Soc. 135 (1988) 25.
[21] K. Watanabe, M. Koseki, N. Kumagai, J. Power Sources 58 (1996) 23.
[22] M. Oshitani, M. Watada, T. Tanaka, T. Iida, in: P.D. Bennett, T. Sakai (Eds.), Hydrogen and Metal Hydride Batteries, PV 94-27, The Electrochemical Society Proceedings Series, Pennington, NJ, 1994, p. 303.
[23] R.M. Bendert, D.A. Corrigan, J. Electrochem. Soc. 136 (1989) 1369.
[24] M. Murthy, G.S. Nagarajan, J.W. Weidner, J.W. Van Zee, J. Electrochem. Soc. 143 (1996) 2319.
[25] D.R. Lide (Ed.), Handbook of Chemistry and Physics, CRC Press, Boca Raton, 1991.
[26] W.D. Johnson, R.C. Miller, R. Mazelsky, J. Phys. Chem. 172 (1984) 235.
[27] S. Kim, D.A. Tryk, M.R. Antonio, R. Carr, D.A. Scherson, J. Phys. Chem. 98 (1994) 10269.
[28] K. Watanabe, T. Kikuoka, N. Kumagai, J. Appl. Electrochem. 25 (1995) 219.

[29] R.E. Carbonio, V.A. Macagno, M.C. Giordano, J.R. Vilche, A.J. Arvia, J. Appl. Electrochem. 12 (1982) 121.
[30] R.E. Carbonio, V.A. Macagno, M.C. Giordano, J.R. Vilche, A.J. Arvia, J. Electrochem. Soc. 129 (1982) 983.
[31] S.I. Cordoba-Torresi, A. Hugot-Le Goff, S. Joiret, J. Electrochem. Soc. 138 (1991) 1554.
[32] J. Chen, D.H. Bradhurst, S.X. Dou, H.K. Liu, J. Electrochem. Soc. 146 (1999) 3606.
[33] E.J. Casey, A.P. Dubois, P.E. Lake, W.J. Moroz, J. Electrochem. Soc. 112 (1965) 371.
[34] R.D. Armstrong, A.K. Sood, M. Moore, J. Appl. Electrochem. 15 (1985) 603.
[35] M.V. Vazquez, R.E. Carbonio, V.A. Macagno, J. Electrochem. Soc. 138 (1991) 1874.
[36] S.I. Córdoba de Torresi, Electrochim. Acta 40 (1995) 1101.